Chem. Senses 39: 295–311, 2014
doi:10.1093/chemse/bjt115
Advance Access publication January 22, 2014

Differential Effects of Bitter Compounds on the Taste Transduction Channels TRPM5 and IP_3 Receptor Type 3

Maarten Gees[1], Yeranddy A. Alpizar[1], Tomas Luyten[2], Jan B. Parys[2], Bernd Nilius[1], Geert Bultynck[2], Thomas Voets[1] and Karel Talavera[1]

[1]Department of Cellular and Molecular Medicine, Laboratory of Ion Channel Research, KU Leuven, B-3000 Leuven, Belgium and [2]Department of Cellular and Molecular Medicine, Laboratory of Molecular and Cellular Signaling, KU Leuven, B-3000 Leuven, Belgium

Correspondence to be sent to: Karel Talavera, Department of Cellular and Molecular Medicine, Laboratory of Ion Channel Research, Herestraat 49, Campus Gasthuisberg, O&N1 Box 802, KU Leuven, B-3000 Leuven, Belgium. e-mail: Karel.talavera@med.kuleuven.be

Accepted December 10, 2013

Abstract

Transient receptor potential cation channel subfamily M member 5 (TRPM5) is a Ca^{2+}-activated nonselective cation channel involved in the transduction of sweet, bitter, and umami tastes. We previously showed that TRPM5 is a locus for the modulation of taste perception by temperature changes, and by quinine and quinidine, 2 bitter compounds that suppress gustatory responses. Here, we determined whether other bitter compounds known to modulate taste perception also affect TRPM5. We found that nicotine inhibits TRPM5 currents with an effective inhibitory concentration of ~1.3 mM at −50 mV. This effect may contribute to the inhibitory effect of nicotine on gustatory responses in therapeutic and experimental settings, where nicotine is often employed at millimolar concentrations. In addition, it implies the existence of a TRPM5-independent pathway for the detection of nicotine bitterness. Nicotine seems to act from the extracellular side of the channel, reducing the maximal whole-cell conductance and inducing an acceleration of channel closure that leads to a negative shift of the activation curve. TRPM5 currents were unaffected by nicotine's metabolite cotinine, the intensive sweetener saccharin or by the bitter xanthines caffeine, theobromine, and theophylline. We also tested the effects of bitter compounds on another essential element of the sweet taste transduction pathway, the type 3 IP_3 receptor (IP_3R3). We found that IP_3R3-mediated Ca^{2+} flux is slightly enhanced by nicotine, not affected by saccharin, modestly inhibited by caffeine, theobromine, and theophylline, and strongly inhibited by quinine. Our results demonstrate that bitter compounds have differential effects on key elements of the sweet taste transduction pathway, suggesting for heterogeneous mechanisms of bitter–sweet taste interactions.

Key words: caffeine, gustatory interaction, nicotine, quinine, sweet, taste mixture

Introduction

Mammalian gustatory perception involves the detection of individual taste qualities (sweet, bitter, salty, sour, and umami) in complex mixtures. This is possible because, by expressing singly tuned molecular receptors, individual taste receptor cells recognize tastants of a single quality (Chandrashekar et al. 2006; Sugita 2006; Chaudhari and Roper 2010). However, it is well known that many tastants "interact" with each other, producing either perceptual potentiation or inhibition (Keast and Breslin 2002). The elucidation of the mechanisms underlying these interactions is, therefore, critical for a comprehensive understanding of taste processing. Mixture interactions may arise at different levels, such as the conscious experience, the central nervous system, the afferent fibers and the gustatory periphery (Lawless 1977; Formaker and Frank 1996; Formaker et al. 1997; Schifferstein 2003; Vandenbeuch et al. 2004; Frank et al. 2005). The peripheral interactions have drawn considerable attention and may arise from various mechanisms. These include chemical interactions between tastant molecules, competition between tastants for a specific receptor, cross-talk between transduction cascades in a single taste receptor cell, lateral cell–cell interactions within the taste buds, and interactions between gustatory signals at the level of the papillae and/or the afferent nerve fibers (Formaker and Frank 1996; Vandenbeuch et al. 2004; Frank et al. 2005).

The recent elucidation of the molecular pathways underlying taste perception allows a more direct identification of molecular loci where taste interactions may take place at the level of taste receptor cells. According to the current model, the transduction of sweet, bitter, and umami taste is initiated upon activation of G-protein-coupled taste receptors, which triggers Ca^{2+} release from the endoplasmic reticulum by type 3 IP_3 receptors (IP_3R3) and the subsequent activation of the Ca^{2+}-activated nonselective cation channel transient receptor potential cation channel subfamily M member 5 (TRPM5) (Liu and Liman 2003; Zhang et al. 2003; Hisatsune et al. 2007; Liman 2007; Zhang et al. 2007). Opening of TRPM5 channels leads to cation influx and depolarization of the taste receptor cell, which is necessary for the communication with afferent gustatory fibers (Huang et al. 2007; Romanov et al. 2007; Zhang et al. 2007). In principle, physical and chemical factors modulating the function of any of these molecular players are expected to alter taste perception. For instance, we have previously shown that heat-induced stimulation of TRPM5 explains the thermal modulation of sweet taste perception (Talavera et al. 2005). In addition, TRPM5 is also modulated by chemical factors, such as phosphatidylinositol 4,5-bisphosphate (Liu and Liman 2003), acidification (Liu et al. 2005), and arachidonic acid (Oike et al. 2006). Furthermore, we have shown in the mouse that the model bitter compounds quinine and quinidine inhibit TRPM5 currents and TRPM5-dependent gustatory nerve responses to sweeteners (Talavera et al. 2008). Hence, this channel constitutes a locus for the peripheral modulation of taste perception.

Interestingly, other bitter compounds of extensive popular use also produce gustatory suppression. Such is the case of nicotine, whose effects on gustatory transduction have drawn significant attention (Simons et al. 2006; Lyall et al. 2007; Tomassini et al. 2007). These studies are in general motivated by the well-known deleterious effects of smoking and tobacco use on taste perception (Grunberg 1982, 1985). It has been shown that oral application of nicotine depresses gustatory neurons in the nucleus of the solitary tract (Simons et al. 2006). Nicotine-induced depression of responses to NaCl and citric acid was proposed to depend on activation of trigeminal nociceptors. On the other hand, nicotine was proposed to modulate chorda tympani responses to salts by interacting directly with the vanilloid receptor TRPV1 and by stimulating the epithelial sodium channel in taste receptor cells (Lyall et al. 2007).

It is notable, however, that the acute effects of nicotine on elements of the sweet transduction cascade(s) have not been tested. Taking into account the role of TRPM5 as a locus for sweet taste modulation (Talavera et al. 2005, 2007, 2008), we here determined whether this channel is targeted by nicotine. We also tested the effects of nicotine's metabolite cotinine, the bitter xanthines caffeine, theobromine and theophylline, and saccharin, an intensive synthetic sweetener that also induces bitter taste. We found that, of all compounds tested, nicotine is the only one able to affect TRPM5, producing current inhibition by decreasing the maximal whole-cell conductance and increasing the rate of channel closure. In addition, we determined whether these bitter compounds affect IP_3R3, which is another essential element of the sweet taste transduction pathway (Hisatsune et al. 2007). We found that this intracellular Ca^{2+}-release channel is slightly stimulated by nicotine, strongly inhibited by quinine, modestly inhibited by caffeine, theobromine and theophylline, and not affected by saccharin.

Taken together, our results demonstrate that bitter compounds have differential effects on key elements of the sweet taste transduction pathway, which suggests heterogeneous mechanisms of bitter–sweet taste interactions. Furthermore, they constitute independent evidence for the existence of TRPM5- and IP_3R-independent pathways for the detection of nicotine and quinine bitterness.

Materials and methods

Transfection and culture of HEK-293 cells

Murine TRPM5 in the pAGGS-IRES-GFP vector was transiently transfected in human embryonic kidney cells (HEK-293) using Trans-IT-293 reagents (Mirus). Cells were seeded in 18-mm glass coverslips coated with poly-L-lysine (0.1 mg/mL) and grown in Dulbecco's modified Eagle's medium containing 10% (v/v) fetal calf serum, 2 mM l-glutamine, 2 U/mL penicillin, and 2 mg/mL streptomycin at 37 °C in humidity-controlled incubator with 10% CO_2.

Patch-clamp experiments

For current recordings, coverslips with cells were placed in the stage of an inverted microscope (Olympus IX70) and rinsed for a few minutes with Krebs (stabilization) solution, containing (in millimolar [mM]): 150 NaCl, 6 KCl, 1 $MgCl_2$, 1.5 $CaCl_2$, 10 glucose, and 10 HEPES and titrated to pH 7.4 with 1 N NaOH. Currents were recorded using the whole-cell patch-clamp technique using an EPC-7 (LIST Electronics) amplifier and filtered with an 8-pole Bessel-filter (Kemo). For control of voltage-clamp protocols and data acquisition, we used an IBM-compatible PC with a TL-1 DMA interface (Axon Instruments) and the software pCLAMP (version 9.0; Axon Instruments). Bath solutions were perfused by gravity via a multibarrelled pipette. Patch pipettes were pulled from Vitrex capillary tubes (Modulohm) using a DMZ-Universal puller (Zeitz-Instruments). An Ag–AgCl wire was used as reference electrode. Adequate voltage control was achieved by using low pipette resistances (1–2.5 MΩ) and series resistance compensation to the maximum extent possible (40–50%). Membrane capacitive transients were electronically compensated. Current traces were filtered at 2.5–5 kHz and digitized at 5–10 kHz.

TRPM5 currents were recorded in the whole-cell patch-clamp configuration, using an extracellular solution containing (in millimolar [mM]): 150 NaCl, 5 $CaCl_2$, 1 $MgCl_2$, and 10 HEPES and was titrated to pH 7.4 with NaOH.

The intracellular (pipette) solution contained (in millimolar [mM]): 50 NaCl, 100 $NMDG^+$, and 10 HEPES and was titrated to pH 7.2 with NaOH. To ensure basal TRPM5 activation, the intracellular solution also contained 500 nM free Ca^{2+} (2 mM EGTA and 1.55 mM $CaCl_2$) (Hofmann et al. 2003; Liu and Liman 2003; Prawitt et al. 2003; Talavera et al. 2005; Ullrich et al. 2005).

Currents were routinely recorded during the application of 300 ms-lasting voltage steps to +100 mV followed by a step to −50 mV. The holding potential was set to +28 mV, which equals the theoretical equilibrium potential for Na^+, the sole TRPM5-permeant ion in the solutions. As a result, no steady TRPM5 current occurred between test pulses, allowing detection of leak currents and avoiding ionic depletion and accumulation in the intracellular milieu (Talavera et al. 2008; Meseguer et al. 2011). All experiments were performed at 25–26 °C.

Patch-clamp data were analyzed using WinASCD (G. Droogmans, KU Leuven) and Origin 7.0 (OriginLab Corporation). Whenever needed, the linear leak component of the current traces was digitally subtracted before data analysis. Time constants of current relaxation (τ) were obtained from the fit of current traces with a single exponential function. For current amplitudes, dose-response curves were fit by a Hill function of the form:

$$Inhibition = \frac{100}{1+(IC_{50}/[D])^{H}}$$

where an effective inhibitory concentration (IC_{50}) is the effective concentration, [D] is the drug concentration, and H is the Hill coefficient. Current–voltage relationships were fit by a linear × Boltzmann-type function:

$$I(V) = \frac{G_{max}(V-V_r)}{1+\exp(-(V-V_{act}/s_{act})}$$

where G_{max} is the maximal TRPM5 whole-cell conductance, V_r the reversal potential, V_{act} is the potential of half-maximal activation, and s_{act} is the slope factor.

Estimation of the concentration of nicotine remaining in cells after brief washout

HEK-293 cells were seeded directly on the surface of a 12-well plate (Greiner) without any coating and grown in a monolayer up to 100% confluence. Cells were incubated with phosphate-buffered saline (PBS) solution containing 10 mM nicotine, then this solution was removed, and cells were washed with fresh PBS for 2 s. Subsequently, cells were incubated twice for 30 min in 500 µL of fresh PBS to allow nicotine to leak out of the cells. The same protocol was performed with nicotine in the absence of cells to determine how much nicotine remains in the cell container after washout, and in the presence of cells without nicotine to determine the possible contribution of cellular components (such as free DNA released from damaged cells) to the absorbance measured at 260 nm. The concentration of nicotine present in the solutions was determined by measuring absorbance at 260 nm in a conventional spectrophotometer (DU640B; Beckman Coulter), as previously described (Clayton et al. 2013). Absolute absorbance values were converted into nicotine concentrations by means of a calibration curve obtained from measurements of absorbance in several samples of known nicotine concentrations (range from 0.01 to 3 mM).

Expression of IP_3R isoforms

The expression levels of IP_3R isoforms were analyzed and quantified exactly as published previously (Missiaen et al. 2004; Thebault et al. 2005). In short, microsomes isolated from Lvec cells were subjected to sodium dodecyl sulfate–polyacrylamide gel electrophoresis and western blotting, and the 3 IP_3R isoforms were assayed using isoform-specific antibodies. We used polyclonal antibodies Rbt03 and Rbt02 against IP_3R1 and IP_3R2, respectively (Parys et al. 1995) and the monoclonal MMAtype3 (#610313; BD Transduction Laboratories) against IP_3R3. Control samples were microsomes from RINm5F insulinoma and RBL-2H3 mucosal mast cells. Detection was performed by fluorimaging using Vistra-ECF (Amersham Biosciences) as substrate (Vanlingen et al. 1997).

Unidirectional $^{45}Ca^{2+}$-flux assay

Unidirectional $^{45}Ca^{2+}$-flux experiments were performed as described elsewhere in full detail (Luyten et al. 2014). Briefly, Lvec cells (Miyawaki et al. 1990) were seeded in 12-well clusters (Greiner) at a density of 6×10^4 cells per well. Experiments were carried out on confluent cell monolayers on the seventh day after seeding. Permeabilization of the plasma membrane was achieved by incubating the cells for 10 min with a solution containing (in millimolar [mM]) 120 KCl, 30 imidazole–HCl (pH 6.8), 2 $MgCl_2$, 1 ATP, 1 EGTA, and 40 µg/mL saponin at 30 °C. The nonmitochondrial Ca^{2+} stores were loaded for 45 min at 30 °C in 120 KCl, 30 imidazole–HCl (pH 6.8), 5 $MgCl_2$, 5 ATP, 0.44 EGTA, 10 NaN_3 to prevent mitochondrial Ca^{2+} uptake and 150 nM of total free Ca^{2+} (including $^{45}Ca^{2+}$ whose concentration is chosen to have a final specific activity of 0.3 MBq/mL). The cells were then washed twice with 1 mL of efflux medium containing (in millimolar [mM]) 120 KCl, 30 imidazole–HCl (pH 6.8), 1 EGTA, and 4 µM thapsigargin to block the sarco/endoplasmic reticulum Ca^{2+}-ATPase (SERCA) Ca^{2+} pumps. The efflux medium was replaced every 2 min during 18 min. After 10 min, cells were challenged with IP_3 (3 µM). At the end of each experiment, the $^{45}Ca^{2+}$ remaining in the stores was released by incubation with 1 mL of a 2% sodium dodecyl sulfate solution for 30 min. The time course of the $^{45}Ca^{2+}$ release was calculated by summing in retrograde order the amount of radioactivity in the cells at the end of the experiment and the radioactivity collected during the successive time intervals.

Drugs

All chemicals were purchased from Sigma-Aldrich. Nicotine was kept in a nitrogen atmosphere to prevent oxidation, and solutions were freshly prepared before the experiments. Cotinine, saccharin, caffeine, theobromine, theophylline, and quinine were weighed and directly added to the solutions.

Statistical analysis

Statistical analyses were performed with Origin 7.0. Data presented as mean ± standard error of the mean. ANOVA and *t*-tests were performed whenever appropriate. $P < 0.05$ was considered as statistical significance.

Results

Nicotine inhibits TRPM5

Extracellular application of nicotine inhibited whole-cell TRPM5 currents in a dose dependent and reversible manner (Figure 1A and B). The inhibition was more pronounced at negative potentials, with IC_{50} values of 1.34 ± 0.10 mM at −50 mV and 3.42 ± 0.09 mM at +100 mV ($n = 5$; Figure 1C). The Hill coefficient was 1.08 ± 0.08 and 0.96 ± 0.03 at −50 mV and +100 mV, respectively.

Notably, both the installation and the reversion of nicotine effects on the TRPM5 current were very quick (Figure 1B). For instance, the potent inhibitory effect of 10 mM nicotine was reversed within 4 s. Considering that the time needed for the exchange of the extracellular solution in our recording conditions is ~2 s, we estimate that the inhibition of TRPM5 is relieved within 1–2 s upon washout. This suggests that nicotine inhibits TRPM5 by acting from the extracellular side of the channel. However, it could be also possible that nicotine acts from the intracellular side, and that it diffuses quickly from the action site(s) upon washout. To distinguish between these possibilities, we set out to estimate the nicotine concentration remaining in the cells after the period of washout that is sufficient for the reversal of the effects on TRPM5 currents. For this, HEK-293 cells were incubated with PBS containing 10 mM of nicotine for 30 s. This solution was removed (Figure 2A; Step 1) and cells were rinsed for 2 s using 500 µL of fresh PBS to simulate the effect of the washout with the perfusion system used in the patch-clamp recordings (Figure 2A; Step 2). Then, cells were incubated twice for 30 min in renewed PBS (Figure 2A; Steps 3 and 4). Samples collected in the 2 last rinsing steps were used to measure absorbance at 260 nm. The concentration of nicotine contained in these samples was determined using a calibration curve obtained from measurements of absorbance in samples of known nicotine concentrations (Figure 2C). As controls, the same protocol was performed with nicotine in the absence of cells and in the presence of cells without nicotine. The results (shown in Figure 2D) clearly demonstrate that 1) in the absence of cells, nicotine is effectively washed out from the container after the first (2 s) rinsing step, 2) cellular components do not contribute significantly to the absorbance, and 3) there is a significant amount of nicotine remaining in the cells after the first (2 s) rinsing step.

We then estimated the concentration of nicotine remaining in the cells after the 2 s period of washout, assuming that nicotine distributes homogeneously. We used the equation: $C_{Cells} = n_{Nic}/V_{Cells}$, where n_{Nic} is the sum of the number of moles of nicotine collected in the rinsing Steps 3 and 4. This was determined from the data shown in Figure 2D with the equation: $n_{Nic} = V_S\left([Nic]^{Cells}_{1st30'} - [Nic]^{No\ cells}_{1st30'} + [Nic]^{Cells}_{2nd30'} - [Nic]^{No\ cells}_{2nd\ 30'}\right)$, where V_S (=500 µL) is the volume of the rinsing solutions in Steps 3 (subscript 1st 30′) and 4 (subscript 2nd 30′), and the superscripts "Cells" and "No cells" denote the nicotine concentrations determined in the presence and in the absence of cells, respectively. V_{Cells} is the volume occupied by the cells and was calculated as the product of the area of the wells (=3.8 cm^2) and the height of the cell monolayer (~25 µm). The calculations gave an estimate C_{Cells} ~10 mM, which indicates that a considerable amount of nicotine accumulates in the cells and remains in them after the period of washout needed for the reversal of the inhibitory effects on the TRPM5 currents. This strongly suggests that nicotine inhibits TRPM5 by acting from the extracellular side.

Effects of nicotine on the gating properties of TRPM5

We further analyzed the effects of nicotine on TRPM5 by determining the voltage dependence of the steady state and kinetic properties of TRPM5 currents in the control and in the presence of 3 mM extracellular nicotine. For this, currents were recorded during the application of a voltage step lasting 300 ms to potentials from −125 to +175 mV followed by a step to −50 mV (Figure 3A). Current–voltage (I/V) relationships determined from the amplitude of steady-state currents at the end of the pre-pulses indicate that nicotine inhibits TRPM5 at all membrane potentials tested (Figure 3B), and that the inhibition was stronger at negative voltages (Figure 3C), consistent with the data in Figure 1. To test whether the voltage dependence of nicotine effects arises from changes in the rectification pattern of open channels, we determined the voltage dependence of instantaneous current amplitudes in control and in the presence of nicotine (Figure 4A and B). The data clearly indicate that this is not the case, as they were well-fitted by a linear function in both cases. In addition, the reversal potential was not significantly different between control (24.4 ± 0.3 mV; $n = 5$) and in the presence of nicotine (24.7 ± 0.5 mV). Thus, the voltage dependence of nicotine-induced inhibition should arise from effects on gating properties. Indeed, although application of 3 mM nicotine had no significant effect on the voltage

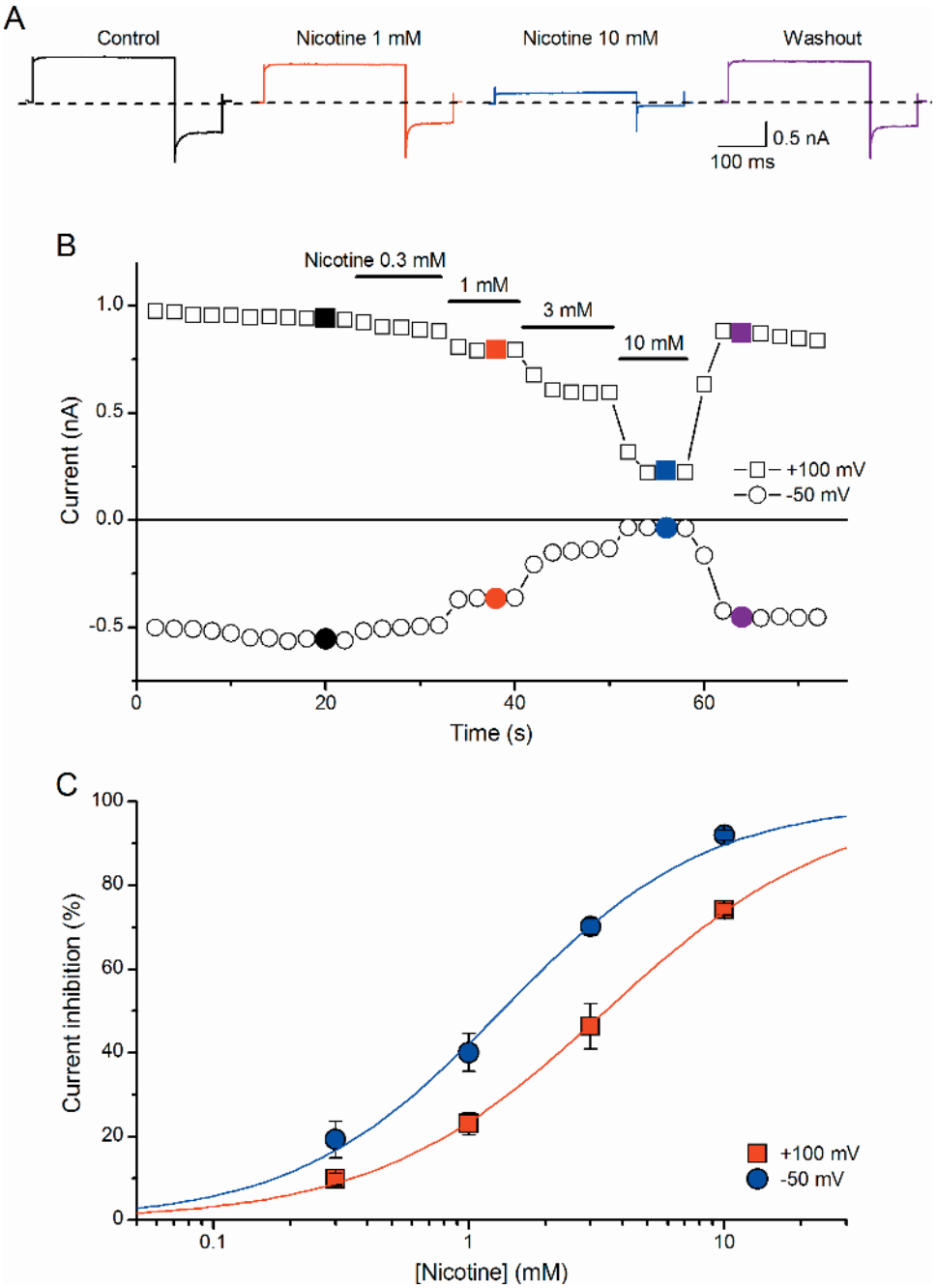

Figure 1 Nicotine inhibits TRPM5 currents in HEK-293 cells. (**A**) TRPM5 currents recorded in the control condition and in the presence of extracellular nicotine (0.3–10 mM). Currents were elicited by applying depolarizing pulses to +100 mV followed by a step to −50 mV (holding potential of +28 mV). The traces correspond to the current amplitudes marked with filled symbols in B. (**B**) Time course of the amplitude of steady-state currents at +100 and −50 mV. Extracellular application of nicotine at different concentrations is denoted by the horizontal bars. (**C**) Concentration-dependent inhibition of TRPM5 currents at +100 and −50 mV (mean ± standard error of the mean, $n = 5$). This figure is reproduced in color in the online version of the issue.

sensitivity of channel activation ($s_{act} = 58 \pm 4$ mV in control compared with $s_{act} = 57 \pm 3$ mV in the presence of nicotine; $n = 5$), it did induce a significant shift of the activation curve to more positive potentials ($V_{act} = 60 \pm 9$ mV in the control conditions compared with $V_{act} = 116 \pm 12$ mV, $P < 0.05$; $n = 5$). Furthermore, nicotine reduced the time constant of current relaxation at negative potentials (Figure 4D), which indicates that it induces an increase of the rate of channel closure.

In addition to the voltage-dependent effect of nicotine on gating kinetics, there was a voltage-independent inhibitory component that was evidenced by a significant decrease of the maximal whole-cell conductance, G_{max}, to $24.2 \pm 6.5\%$ of control values (Figure 3C; $P < 0.05$; $n = 5$).

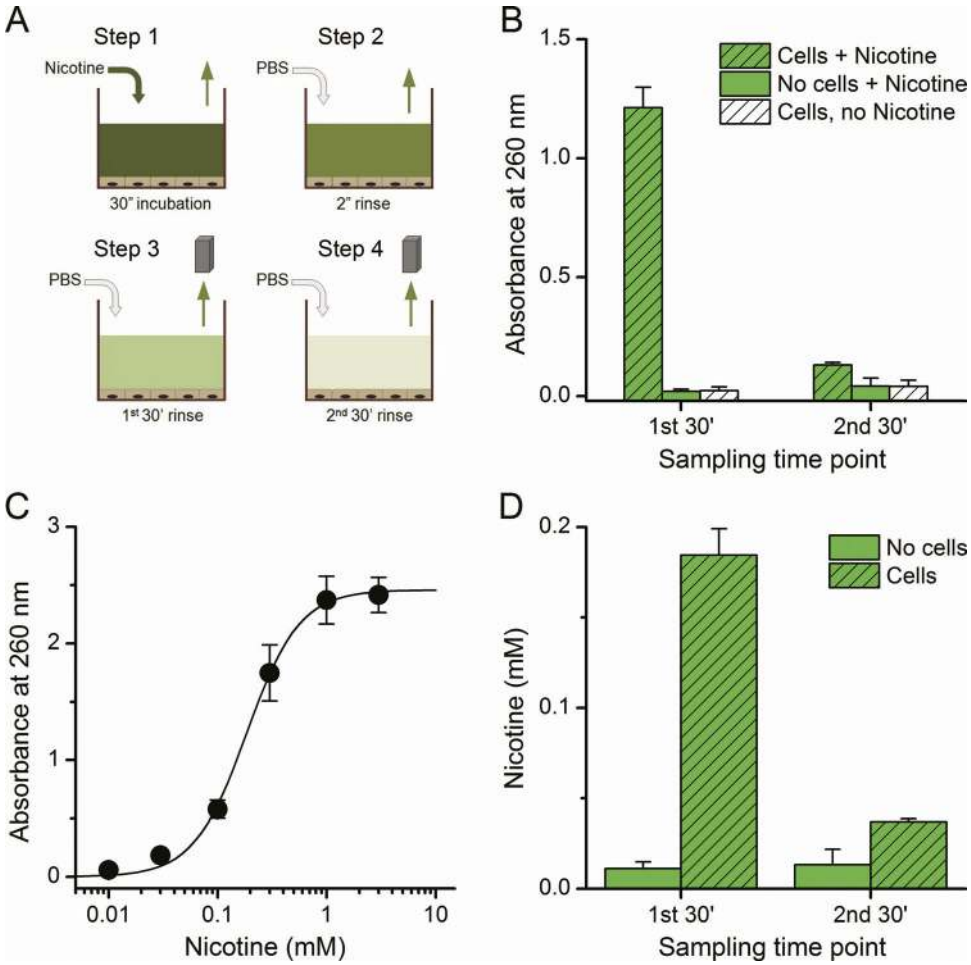

Figure 2 Estimation of the intracellular nicotine concentration remaining in cells after extracellular washout. (**A**) Schematic representation of the experimental procedure used to determine the concentration of nicotine that remains in cells after a period of washout that is sufficient for the reversal of inhibition of TRPM5 currents. Step 1: incubation of nicotine; Step 2: 2 s washout with PBS, Steps 3 and 4: 30 min washes with PBS. (B) Absolute values of spectrophotometric ultraviolet absorbance detected in the PBS solutions collected in successive rinsing steps (panel A: Steps 3 and 4). The bars represent mean ± standard error of the mean (n = 4). (**C**) Standard curve for the absorbance detected at 260 nm in solutions containing nicotine. The line represents the fitting with a Hill function characterized by a maximal absorbance of 2.46 ± 0.05, a nicotine concentration for half-maximal absorbance of 184 ± 12 μM and a Hill coefficient of 1.8 ± 0.2. (**D**) Nicotine concentration in the PBS solutions collected in successive rinsing steps (panel A: Steps 3 and 4). The bars indicate mean ± standard error of the mean (n = 4). This figure is reproduced in color in the online version of the issue.

Nicotine's metabolite cotinine does not inhibit TRPM5

In the body, nicotine is quickly metabolized to cotinine, a bitter alkaloid that is also present in tobacco and that is used as a biomarker for smoking in humans (Haufroid and Lison 1998). It is therefore possible that some of the effects of nicotine on taste perception are actually produced by cotinine. Thus, we determined the effect of cotinine on TRPM5 currents. In contrast to nicotine, cotinine did not induce significant effects in TRPM5 currents even at the high concentration of 10 mM (Figure 5).

Saccharin and xanthines have no effect on TRPM5

Next, we tested whether other membrane-permeable bitter compounds known to interact with sweet taste transduction may affect TRPM5. Saccharin is an intensive artificial sweetener that produces bitter taste and that has been shown to suppress sweetness intensity ratings in humans (Schiffman et al. 1995). We found that extracellular application of 1 mM saccharin induced no significant change in the amplitude of TRPM5 currents (−0.3 ± 1.5%; Figure 6A). Similarly, neither caffeine, a prominent inhibitor of sweet taste perception (Calviño et al. 1990; Mojet et al. 2004), nor the chemically related xanthines theophylline and theobromine induced changes on the TRPM5 currents (0.1 ± 1.8%, −0.4 ± 3.7%, and 0.5 ± 3.3%; Figure 6B).

Differential effects of bitter compounds on IP_3R-mediated Ca^{2+} release

It has been shown that the IP_3R3 channels are key mediators of the perception of sweet, bitter, and umami

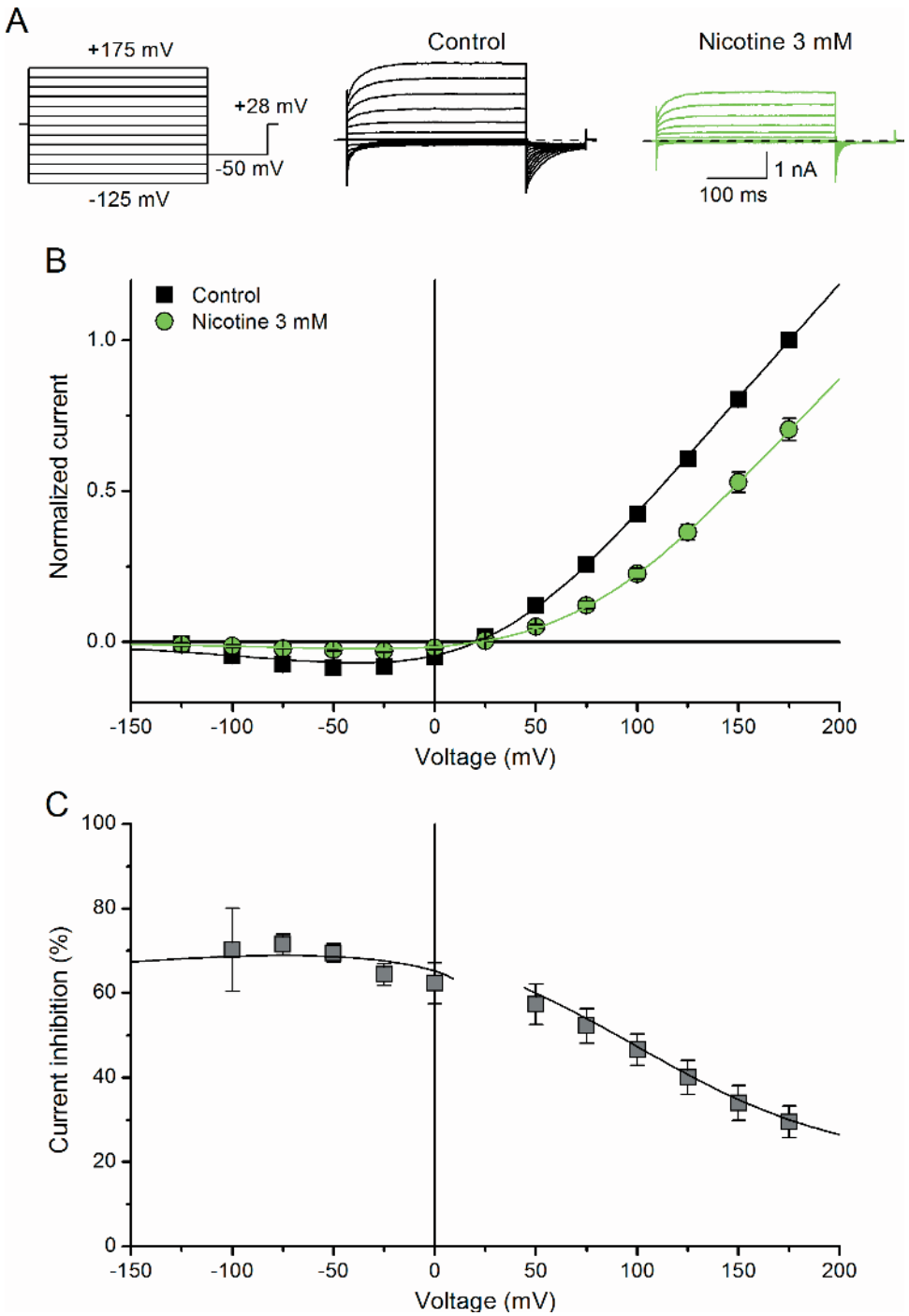

Figure 3 Voltage dependency of TRPM5 current inhibition by nicotine. (**A**) Left panel: voltage protocol used to determine the activation and kinetic properties of TRPM5. Middle and right panels: current traces recorded during the application of this protocol in the control conditions and in the presence of 3 mM extracellular nicotine. (**B**) Average current–voltage relationship of TRPM5 in the control and 3 mM nicotine conditions (n = 5). For each cell, data were normalized to the current value obtained in the control condition at +175 mV. Lines represent the fit of the data with a linear × Boltzmann-type function (see Materials and methods). (**C**) Voltage dependency of current inhibition during the application of 3 mM nicotine. The line was obtained by calculating the voltage dependence of current inhibition from the fit function shown in B (the discontinuity around +25 mV is caused by the slight difference in reversal potential). This figure is reproduced in color in the online version of the issue.

stimuli (Hisatsune et al. 2007) and are proposed to provide the increase in intracellular Ca^{2+} concentration needed for the activation of TRPM5 (Liu and Liman 2003; Zhang et al. 2003;Hisatsune et al. 2007; Liman 2007; Zhang et al. 2007). Thus, it is conceivable that bitter compounds modulate the perception of taste by modulating IP_3R3. To test this possibility, we determined the effects of nicotine, caffeine, theobromine, theophylline, saccharin, and quinine on the

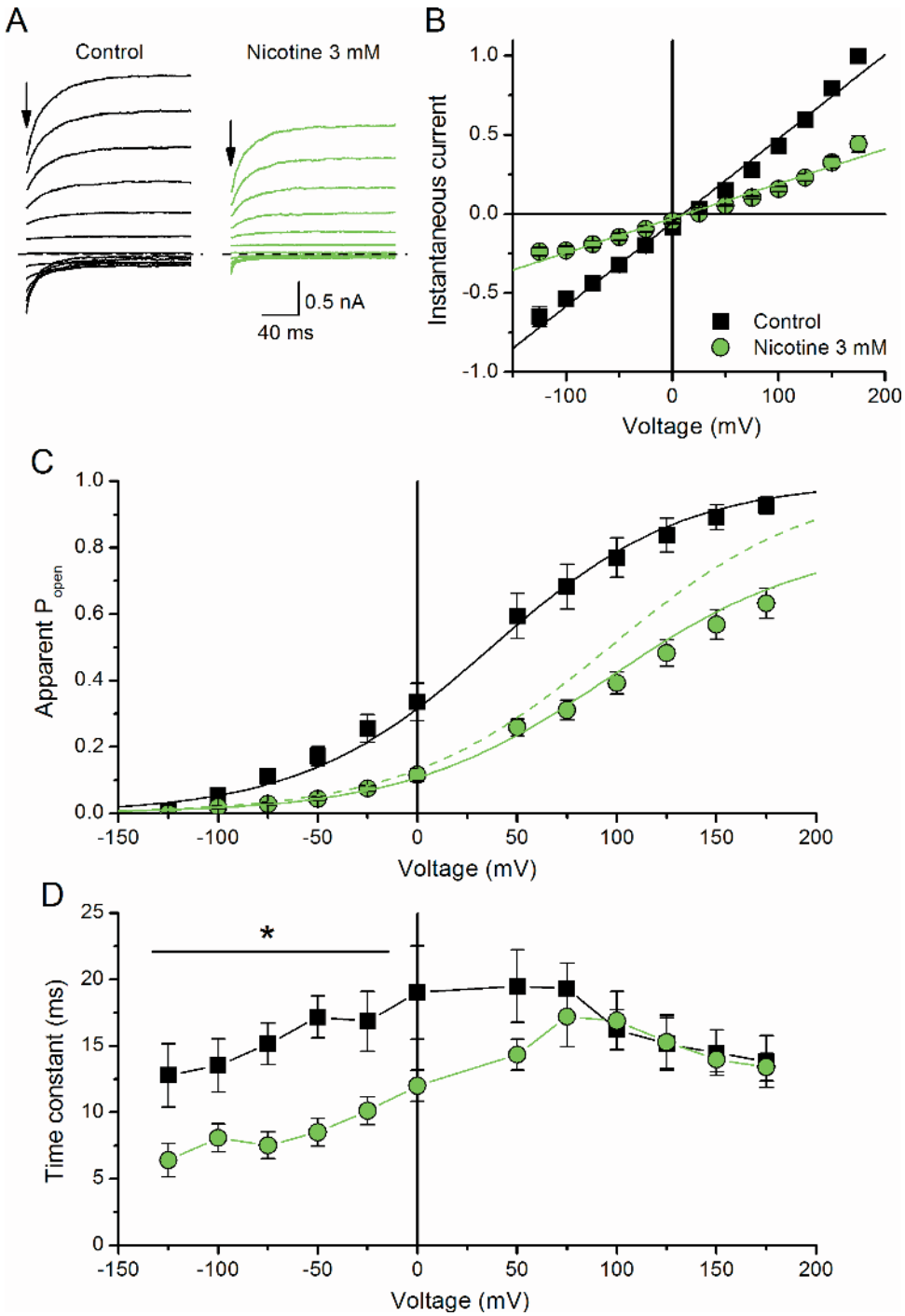

Figure 4 Effect of nicotine on the gating properties of TRPM5. (**A**) The relaxation time course of currents (elicited by the protocol shown in Figure 2A) was fit for each test potential with a single exponential function. The arrows indicate the time point at which instantaneous current amplitudes were determined (see B). (**B**) Instantaneous current amplitudes as a function of the test potential in the control conditions and in the presence of 3 mM nicotine (n = 5). These values were obtained by extrapolating the fit of the current traces to the beginning of the pulse (see arrow in A) and were normalized to the value at +175 mV in the control for each cell. Both voltage dependencies were well fit by linear functions. The slope of the linear dependence in the presence of 3 mM nicotine amounts to 53% of that of control. (**C**) Effects of 3 mM extracellular nicotine on the voltage dependence of activation (normalized whole-cell TRPM5 conductance). Data were obtained by fitting the tail currents with a single exponential and normalizing to the maximal conductance (G_{max}) obtained in control. Continuous lines are the Boltzmann function calculated with the values of voltage half-maximal activation (V_{act}) and slope factor (s_{act}) determined in each condition. The dashed line represents the rescaled Boltzmann function obtained in nicotine, illustrating that nicotine shifted the activation curve to more positive potentials while not affecting its slope. (**D**) Voltage dependence of the average time constant of current relaxation in the control condition and in the presence of 3 mM nicotine (n = 5). The horizontal bar and * mark the voltages at which nicotine had a significant effect ($P < 0.05$). This figure is reproduced in color in the online version of the issue.

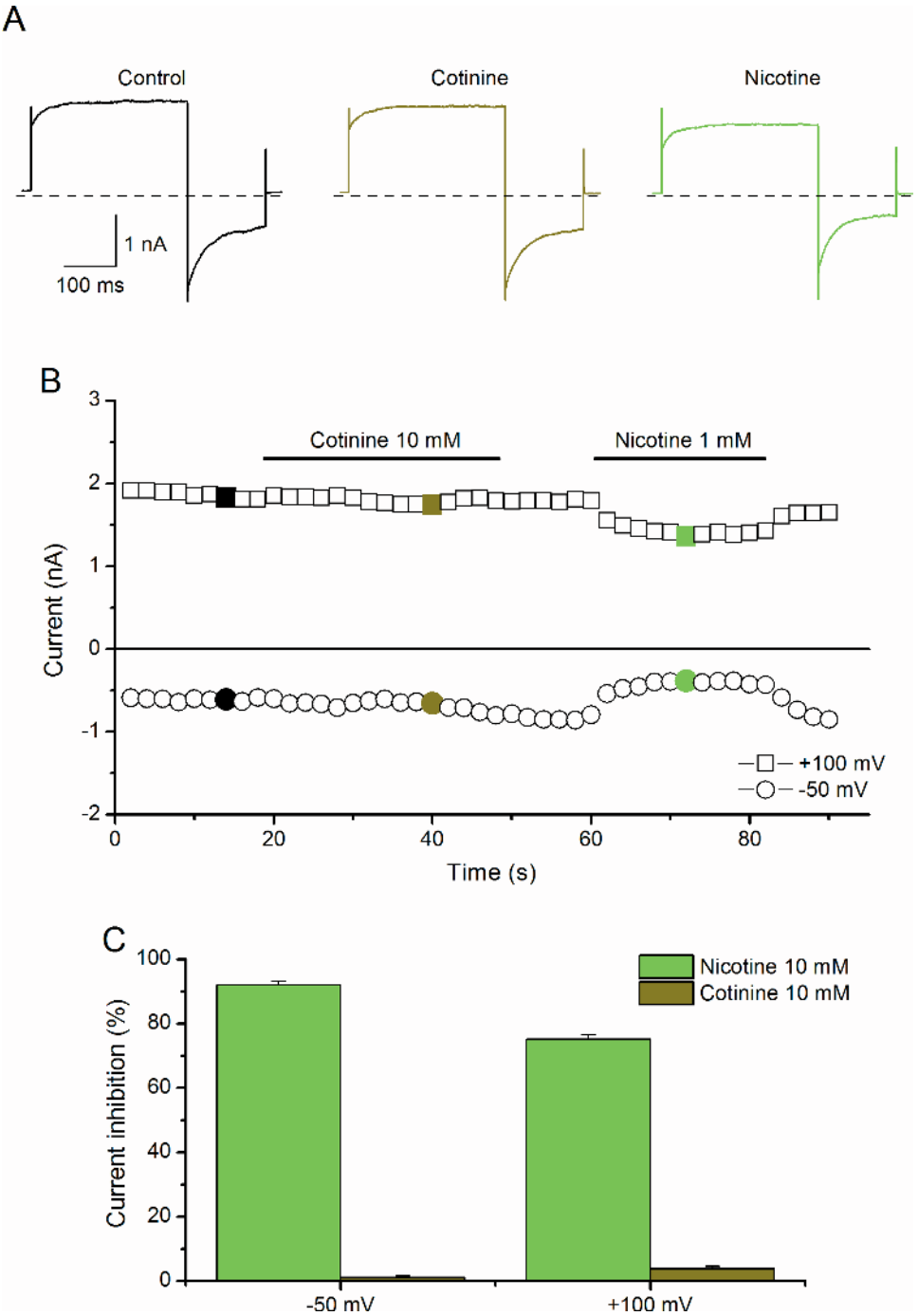

Figure 5 Cotinine has no effect on TRPM5 currents. (**A**) TRPM5 currents recorded in control conditions and in the presence of extracellular cotinine (10 mM) or nicotine (1 mM). Currents were elicited by applying depolarizing pulses to +100 mV followed by a step to –50 mV (holding potential +28 mV). (**B**) Time course of the amplitude of steady-state currents at +100 and –50 mV. Extracellular application of cotinine (10 mM) and nicotine (1 mM) is denoted by the horizontal bars. (**C**) Effect of cotinine (10 mM) and nicotine (10 mM) on TRPM5 currents (mean ± standard error of the mean, $n = 6$). This figure is reproduced in color in the online version of the issue.

properties of the IP_3R using a unidirectional $^{45}Ca^{2+}$-flux assay in saponin-treated plasma membrane-permeabilized Lvec cells. We used these cells because they show a high expression level of IP_3R3 compared with that of the other IP_3R isoforms. Indeed, by using isoform-specific antibodies, we demonstrate that Lvec cells only express IP_3R1 and IP_3R3 (Figure 7). Moreover, quantification of their relative levels was performed by comparison with RBL-2H3 mucosal mast cells, which were previously shown to express all 3 IP_3R isoforms in a proportion IP_3R1:IP_3R2:IP_3R3 10%:70%:20%

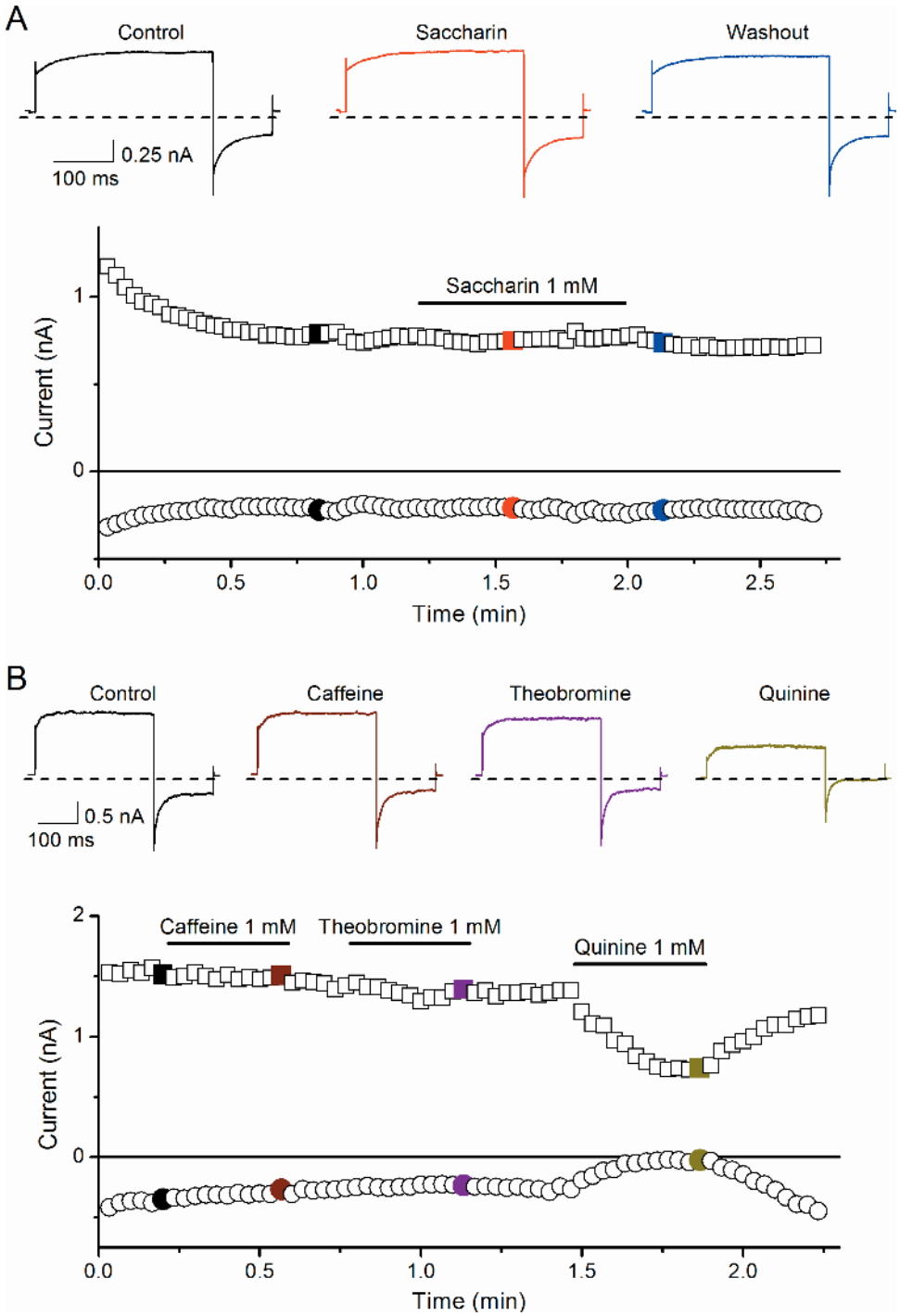

Figure 6 TRPM5 is not affected by saccharin or by bitter xanthines. TRPM5 currents recorded in control conditions and during extracellular application of 1 mM saccharin (**A**), and 1 mM of the xanthines theophylline, caffeine, and theobromine (**B**). Currents were elicited by applying depolarizing pulses to +100 mV followed by a step to −50 mV (holding potential +28 mV). Quinine (1 mM) was used as a positive control. The upper traces correspond to the current amplitudes marked with filled symbols in the lower graph and extracellular application of the chemicals is denoted by the horizontal bars. This figure is reproduced in color in the online version of the issue.

(Wilson et al. 1998). Calculations demonstrated that Lvec cells displayed an IP_3R1:IP_3R3 ratio of 24%:76%, indicating a 3-fold higher level of IP_3R3 compared with IP_3R1. The absence of detectable IP_3R2 is not related to the high expression levels of IP_3R3, as in RINm5F cells, which also express a high level of IP_3R3, the 3 IP_3R isoforms could be detected in a ratio 4%:8%:87%.

In these experiments, the nonmitochondrial Ca^{2+} stores were loaded to steady state with $^{45}Ca^{2+}$. After incubation with 4 µM of thapsigargin, the efflux of $^{45}Ca^{2+}$ was followed

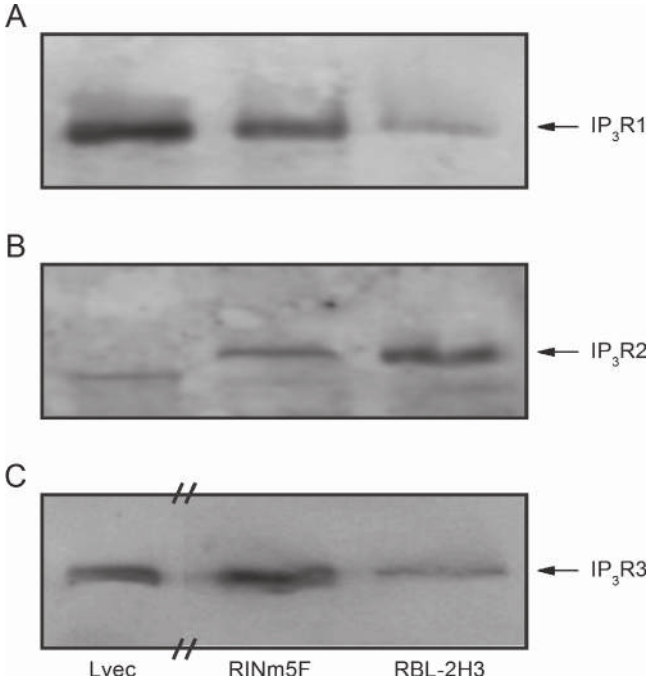

Figure 7 IP_3R isoform expression levels. IP_3R analysis was performed with isoform-specific antibodies against IP_3R1 (**A**. Rbt03 1/1000), IP_3R2 (**B**. Rbt02 1/200), or IP_3R3 (**C**. MMAtype3 1/1000). Lanes were loaded as indicated with microsomes from Lvec cells (A and C: 50 µg/lane; B: 75 µg/lane), RIN5F cells (A and B: 100 µg/lane; C: 50 µg/lane), or RBL-2H3 mucosal mast cells (A: 75 µg/lane; B: 50 µg/lane; C: 100 µg/lane). Only the relevant parts of the gels are shown. Arrows indicate the position of the various IP_3R isoforms. Result typical for 3 independent experiments.

in the presence of 1 mM EGTA. The data were plotted as the Ca^{2+} content as a function of time (Figure 8A) and as the fractional loss (the amount of Ca^{2+} leaving the store in a 2-min time period divided by the total store Ca^{2+} content at that time) as a function of time (Figure 8B). The Ca^{2+} content of the stores gradually decreased over time, whereas adding IP_3 (3 µM) strongly accelerated this decrease in Ca^{2+} content by activating IP_3-induced Ca^{2+} release (Figure 8A). This is observed as a steep increase in the fractional loss (Figure 8B). Importantly, incubation with different nicotine concentrations (ranging from 0.03 to 1 mM) did not suppress IP_3R-mediated Ca^{2+} release, but rather slightly increased it.

Similar results were obtained with saccharin (1 mM), in the presence of which the IP_3R-mediated Ca^{2+} release was not different than in control condition (Figure 9A). Caffeine, theobromine, and theophylline (1 mM) induced a modest reduction of the Ca^{2+} release induced by IP_3 ($18 \pm 1\%$, $26 \pm 1\%$, and $34 \pm 4\%$, respectively). In contrast, quinine produced a dramatic decrease in IP_3-induced Ca^{2+} release at this concentration (Figure 9B). More detailed analysis of quinine effects on IP_3Rs revealed a concentration-dependent response, with an IC_{50} of 150 ± 20 µM and a corresponding Hill coefficient of 1.4 ± 0.2 (Figure 9B inset).

Discussion

TRPM5 and IP_3R3 are crucial elements of the signaling pathways leading to the perception of sweet, bitter, and umami tastes (Zhang et al. 2003; Damak et al. 2006; Hisatsune et al. 2007; Romanov et al. 2007). Considering that TRPM5 channel was shown to be a site of action of quinine and quinidine leading to the inhibition of sweet taste, we here tested whether other bitter compounds known to inhibit sweet taste perception affect TRPM5 and/or the IP_3R3.

Given the long-standing interest on the effects of nicotine on gustatory transduction (Grunberg 1982, 1985; Simons et al. 2006; Lyall et al. 2007; Tomassini et al. 2007), we used this compound as starting point of this study. Although the most powerful effects of nicotine take place at the central nervous system, it has been shown that the peripheral sensory stimulation of nicotine is also important for the regulation of smoke intake and the modulation of craving, thus showing the importance of these peripheral pathways (Rose et al. 1993; Pritchard et al. 1996). However, research on this subject remains scarce, and the mechanisms underlying the influences of nicotine on taste perception seem to be quite complex and still not well understood. Indeed, in addition to inducing bitter taste, nicotine is also known to influence the perception of other tastants. This was first reported for sweet taste as a reduced preference for sweeteners was shown both in smokers and in rats pretreated with nicotine (Grunberg 1982). Furthermore, this was accompanied by a reduced uptake of (high-caloric) sweet foods (Grunberg 1985). Later, it was shown that smoking increased the taste threshold for the other basic tastes salty, sour, and bitter (Sato et al. 2002). The exact way nicotine acts on the perception of these tastes is still not well understood, but very likely multiple different mechanisms are involved. These mechanisms can be situated both at a peripheral level and at an upstream, central level. At the peripheral level, it has been shown that prolonged nicotine treatment reduces the size of fungiform papillae and the number of taste cells (Tomassini et al. 2007). Furthermore, at concentrations larger than 15 mM, nicotine inhibits chorda tympani responses of the taste receptor cells to KCl and NaCl. This was explained by a direct effect of nicotine on TRPV1t, a constitutively active nonselective cation channel derived from the TRPV1 gene, present in the apical membrane of fungiform taste receptor cells (Lyall et al. 2007). In addition to the effects mediated by the gustatory nerves, also trigeminal nociception can play a role in nicotine–taste interactions. Indeed, it has been shown that nicotine suppresses gustatory responses of neurons in the nucleus of the solitary tract and that this effect is strongly reduced after trigeminal ganglionectomy, indicating a central mechanism (Simons et al. 2006). In addition, nicotine can inhibit voltage-dependent sodium channels, and it can sensitize TRPV1 for activation by capsaicin in trigeminal ganglion neurons (Liu et al. 2004). Furthermore, more recently, it was shown that

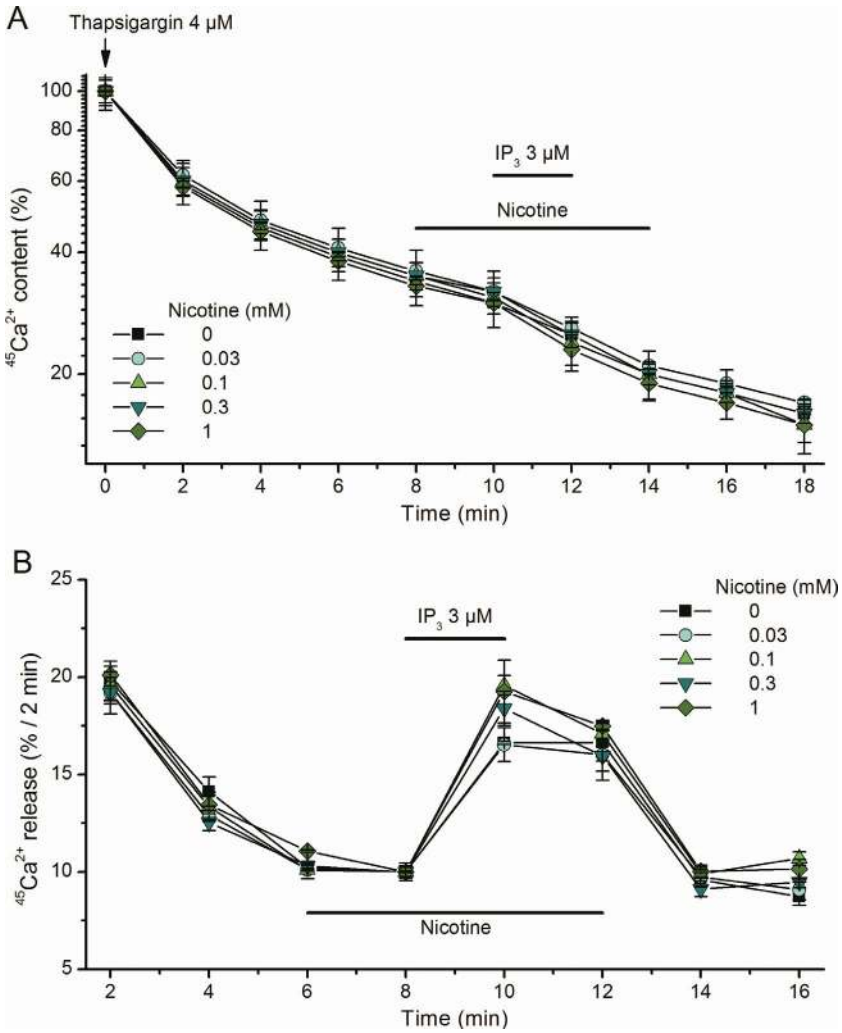

Figure 8 Nicotine does not inhibit IP_3R-mediated Ca^{2+} release. Ca^{2+}-release properties of IP_3R assessed during unidirectional $^{45}Ca^{2+}$-efflux conditions in plasma membrane-permeabilized fibroblasts in which the nonmitochondrial Ca^{2+} stores were loaded with $^{45}Ca^{2+}$ to steady state. At the beginning of the experiment, thapsigargin was added to block SERCA Ca^{2+}-uptake activity. (**A**) Unidirectional $^{45}Ca^{2+}$ fluxes plotted as normalized $^{45}Ca^{2+}$ content (content at time 0 min was set as 100%) as a function of time (min). Ca^{2+} release was activated by 3 µM IP_3 in the absence or presence of different nicotine concentrations added 2 min before IP_3, during IP_3 challenge, and 2 min after IP_3. The values were obtained from 2 replicates. (**B**) Same experiment as in panel A, but Ca^{2+} release was plotted as fractional loss (%/2 min) as a function of time. Nicotine did not inhibit the IP_3R-mediated Ca^{2+} flux. This figure is reproduced in color in the online version of the issue.

nicotine can directly activate TRPA1 (Talavera et al. 2009), a broadly tuned chemo-nocisensor in trigeminal ganglia.

Our present results suggest for another peripheral mechanism of inhibition of gustatory perception, whereby nicotine directly inhibits TRPM5, a key signal transduction channel in the detection of sweet, bitter, and umami tastes. We found this inhibition to be reversible and dose dependent, with an IC_{50} of 1.3 mM at −50 mV. It is important to notice that nicotine concentrations in the millimolar range are not reached during normal smoking, but they may be attained locally during tobacco chewing, the use of the Scandinavian snuss, and in nicotine-replacement therapies (nicotine chewing gum and lozenges). Moreover, our results are especially relevant for the interpretation of experimental studies that have employed nicotine concentrations of up to 600 mM (Carstens et al. 1998; Boucher et al. 2003; Simons et al. 2006).

Interestingly, both the installation and reversion of the inhibitory effect of nicotine on the TRPM5 currents occurred within ~2 s, whereas a considerable amount of nicotine remains in the cells after this washout period. The latter finding is in agreement with the high partition of nicotine in hydrophobic phases (Banyasz 1999). Thus, we propose that nicotine inhibits TRPM5 by acting from the extracellular side of the channel. For the same reasons, we propose that the inhibitory effects are caused directly by nicotine and not via secondary effects caused by the drug, which would not revert within seconds.

The fast effect of nicotine on TRPM5 contrasts sharply with the actions of quinine (Talavera et al. 2008 and present results) and quinidine (Talavera et al. 2008). Indeed, these drugs induce strong inhibitory effects, but the installation and reversal are much slower than for nicotine (~30 s)

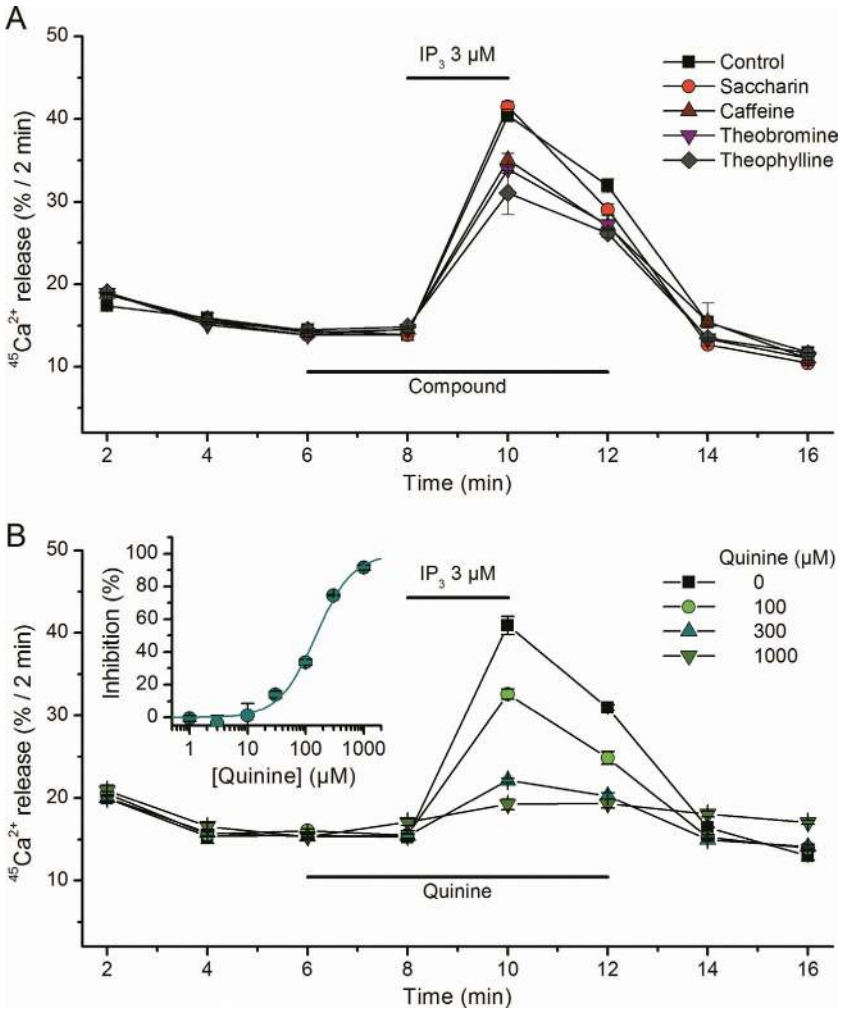

Figure 9 Effects of several bitter compounds on IP_3R-mediated Ca^{2+} release. (**A**) IP_3 (3 μM)-induced Ca^{2+} release measured in the presence of 1 mM saccharin, caffeine, theobromine, and theophylline (plotted as fractional loss, %/2 min). (**B**) Concentration-dependent effect of quinine on the Ca^{2+} release induced by IP_3 (3 μM). The inset shows the quantification of the inhibitory action. The solid line represents the fit of the experimental data by a Hill function. This figure is reproduced in color in the online version of the issue.

(Talavera et al. 2008, Figure 5B). Considering that quinine and quinidine are membrane permeable, it seems likely that they inhibit TRPM5 by acting at the intracellular side of the channel (or membrane). Alternatively, these compounds could act at the extracellular side, with very low on and off rates. At present, we do not have direct evidence that could help excluding any of these possibilities. Nevertheless, the facts that quinine and quinidine have very similar effects on the TRPM5 homolog TRPM4, and that they act quite quickly when applied to the intracellular side of inside-out patches (Talavera et al. 2008) seem to point to an intracellular site of action.

We further investigated the effects of nicotine on TRPM5 and found that the inhibition has 2 components: a voltage-independent component that is characterized by a decrease of the maximal whole-cell conductance and a voltage-dependent component that entails a negative shift of the voltage dependence of activation. An analysis of the whole-cell current kinetics yielded that nicotine induces specifically an increase of the rate of channel closing but does not affect the rate of channel opening. These effects are very similar to those induced by quinine (Talavera et al. 2008) and indicate that these compounds destabilize the open conformation of TRPM5, while leaving the stability of the closed conformation largely unaffected.

Interestingly, application of a high concentration of cotinine, a compound to which nicotine is quickly metabolized *in vivo*, had no significant effect on TRPM5 currents. This suggests that a nicotine-induced inhibition of TRPM5-mediated gustatory responses in the periphery would result from the action of this compound and not through its main oxidation product. In addition, the inefficacy of cotinine also suggests that disruption of nicotine's methyl-pyrrolidine moiety by oxidation abrogates the ability of the molecule to inhibit TRPM5 channels. In future studies, it would be interesting to determine whether methyl-pyrrolidine alone has an inhibitory effect on TRPM5.

Besides shedding light on the mechanisms underlying bitter–sweet taste interactions, the effects of nicotine on TRPM5 have important implications for our understanding of the mechanisms of bitter taste transduction. Our data demonstrate that nicotine inhibits TRPM5 currents and therefore indicate that the perception of the bitter taste of this compound cannot be mediated solely by the TRPM5 pathway. At least one alternative pathway must come into play to trigger the aversive behavior toward nicotine at high concentrations. Accordingly, it has been recently shown that in addition to the TRPM5-dependent pathway, which is common to other bitter compounds such as quinine, nicotine also activates a nAChR-dependent and TRPM5-independent gustatory pathway (Oliveira-Maia et al. 2009).

We tested whether TRPM5 is modulated by other bitter compounds known to have an influence in sweet taste perception. For instance, saccharin is well known to elicit sweet taste, with a threshold concentration of 0.01 mM for activation of T1R2/T1R3 receptors (Li et al. 2002), and to produce bitter and "metallic" tastes (Helgren et al. 1955; Horne et al. 2002). The bitter taste of saccharin can be detected by humans at concentrations as low as 0.4 mM (Horne et al. 2002). This has been attributed to activation of the bitter receptors hTAS2R43 and hTAS2R44, which occur with threshold concentrations of 0.17 and 0.08 mM, respectively (Kuhn et al. 2004). The "metallic" taste sensation has been attributed to TRPV1 activation, which occurs at concentrations above 0.1 mM (Riera et al. 2007). Interestingly, according to Riera et al. (2008), T1R3 knockout mice show aversion to saccharin above 1 mM, and actually a close inspection of their data suggests that aversion is also observed at 0.1 mM. It has been suggested that artificial sweeteners alter intracellular signaling pathways after diffusion into taste receptor cells (Peri et al. 2000; Riera et al. 2007). Our results show that, even at the high concentration of 1 mM, saccharin does not affect TRPM5 current, which indicates that the complex taste properties of this compound are not due to a direct interaction with TRPM5.

Another bitter compound known to inhibit sweet taste perception (Calviño et al. 1990; Mojet et al. 2004) and to interact with several chemosensory mechanisms is caffeine. It has been shown that, in taste receptor cells, caffeine inhibits outwardly and inwardly rectifying K^+ currents and increases intracellular Ca^{2+} in an intracellular store-dependent manner (Zhao et al. 2002). Furthermore, it has been shown that caffeine activates mouse TRPA1, which raises the possibility that this compound may also modulate taste through a trigeminal-dependent pathway. Notably, this mechanism may be only active in mice, as caffeine did not activate human TRPA1 or *Drosophila* TRPA1 (Nagatomo and Kubo 2008; Kim et al. 2010). Here, we tested whether the inhibitory effect of caffeine on sweet taste could be attributed to TRPM5. In contrast to quinine (Talavera et al. 2008) and nicotine (present results), caffeine and the related xanthines theophylline and theobromine had no effect on TRPM5 currents.

Finally, we tested whether bitter compounds are able to interact with other essential element of the sweet gustatory pathway, the IP_3R type 3 (Hisatsune et al. 2007). For this we used Lvec cells, which we here demonstrate to display a high relative expression of IP_3R3 compared with IP_3R1 and IP_3R2 (Figure 7). We found that at concentrations as high as 1 mM, nicotine and saccharin do not compromise the ability of IP_3R3 to mediate Ca^{2+} release upon stimulation with IP_3. At the same concentration, caffeine, theophylline, and theobromine induced a modest reduction of the function of these channels (18–34%). Caffeine and theophylline are well-documented low-affinity (IC_{50} ~20 mM) inhibitor of IP_3R channels (Brown et al. 1992; Bezprozvanny et al. 1994; Missiaen et al. 1994), primarily by acting at the level of the adenine-nucleotide-binding sites of the IP_3R channels, including the IP_3R3 (Bultynck et al. 2003).

On the other hand, quinine induced a very strong inhibition, characterized by an IC_{50} of ~50 μM. The inhibitory effects of quinine on IP_3-induced Ca^{2+} release has been previously reported in murine peritoneal macrophages (Misra et al. 1997) and in dog brain microsomes (Palade et al. 1989). The relative expression of IP_3R3 in those preparations was not reported, but from previous work, it is known that macrophages predominantly express IP_3R2, whereas brain predominantly expresses IP_3R1. Nevertheless, the latter study reported an IC_{50} value (110 μM) that is in the same order of magnitude of the one found here, suggesting that the various IP_3R isoforms are about equally sensitive to quinine. It is also interesting to note that the IC_{50} reported for the inhibition of TRPM5 currents recorded at −50 mV (50 μM; Talavera et al. 2008) is lower than those for IP_3R3 (150 μM; present results) and for the voltage-gated Na^+ channels in rat taste receptor cells (64 μM; Chen and Herness 1997). This suggests that, within the TRPM5 signaling pathway, this is the excitatory channel that is most sensitive to quinine.

Taken together, our results demonstrate that bitter compounds known to inhibit sweet taste perception have differential effects on key elements of the sweet taste transduction pathway, supporting the hypothesis of multiple mechanisms of bitter–sweet taste interactions. Furthermore, our results suggest that nicotine, quinine, and quinidine may also interfere with the perception of bitter and umami, but in as much as the perception of these qualities depends on TRPM5 and IP_3R3 for each particular compound (see Talavera et al. 2008). In fact, our data constitute independent evidence for the existence of TRPM5- and IP_3R3-independent pathway(s) for the detection of quinine and nicotine bitterness. We note that our findings were obtained using heterologous systems and/or cell lines, and thus need to be confirmed in intact taste cells and tissues. Nonetheless, we underscore the importance of the detailed study of the pharmacological properties of individual compounds for the comprehensive understanding of their specific chemosensory properties.

Funding

This work was supported by grants from the Belgian Federal Government [IUAP P7/13], the Research Foundation-Flanders (F.W.O.) [G.0565.07, G.0686.09, and G.A022.11N], and the Research Council of the KU Leuven [GOA 2009/07, EF/95/010, and PFV/10/006). M.G. was supported by a doctoral fellowship from the F.W.O.

Acknowledgments

We would like to thank Melissa Benoit, Marina Crabbe, and Anja Florizoone for the maintenance of the cell cultures. We are also grateful to Dr K. Mikoshiba (Laboratory for Developmental Neurobiology, RIKEN Brain Science Institute, Wako, Japan) for providing the Lvec cells.

References

Banyasz JL. 1999. The physical chemistry of nicotine. In: Gorrod JW, Jacob P 3rd, editors. Analytical determination of nicotine and related compounds and their metabolites. Amsterdam, The Netherlands: Elsevier B.V. p. 149–190.

Bezprozvanny I, Bezprozvannaya S, Ehrlich BE. 1994. Caffeine-induced inhibition of inositol(1,4,5)-trisphosphate-gated calcium channels from cerebellum. Mol Biol Cell. 5(1):97–103.

Boucher Y, Simons CT, Cuellar JM, Jung SW, Carstens MI, Carstens E. 2003. Activation of brain stem neurons by irritant chemical stimulation of the throat assessed by c-fos immunohistochemistry. Exp Brain Res. 148(2):211–218.

Brown GR, Sayers LG, Kirk CJ, Michell RH, Michelangeli F. 1992. The opening of the inositol 1,4,5-trisphosphate-sensitive Ca^{2+} channel in rat cerebellum is inhibited by caffeine. Biochem J. 282:309–312.

Bultynck G, Sienaert I, Parys JB, Callewaert G, De Smedt H, Boens N, Dehaen W, Missiaen L. 2003. Pharmacology of inositol trisphosphate receptors. Pflugers Arch. 445(6):629–642.

Calviño AM, García-Medina MR, Cometto-Muñiz JE. 1990. Interactions in caffeine-sucrose and coffee-sucrose mixtures: evidence of taste and flavor suppression. Chem Senses. 15(5):505–519.

Carstens E, Kuenzler N, Handwerker HO. 1998. Activation of neurons in rat trigeminal subnucleus caudalis by different irritant chemicals applied to oral or ocular mucosa. J Neurophysiol. 80(2):465–492.

Chandrashekar J, Hoon MA, Ryba NJ, Zuker CS. 2006. The receptors and cells for mammalian taste. Nature. 444(7117):288–294.

Chaudhari N, Roper SD. 2010. The cell biology of taste. J Cell Biol. 190(3):285–296.

Chen Y, Herness MS. 1997. Electrophysiological actions of quinine on voltage-dependent currents in dissociated rat taste cells. Pflugers Arch. 434(3):215–226.

Clayton PM, Vas CA, Bui TT, Drake AF, McAdam K. 2013. Spectroscopic studies on nicotine and nornicotine in the UV region. Chirality. 25(5):288–293.

Damak S, Rong M, Yasumatsu K, Kokrashvili Z, Pérez CA, Shigemura N, Yoshida R, Mosinger B Jr, Glendinning JI, Ninomiya Y, *et al.* 2006. Trpm5 null mice respond to bitter, sweet, and umami compounds. Chem Senses. 31(3):253–264.

Formaker BK, Frank ME. 1996. Responses of the hamster chorda tympani nerve to binary component taste stimuli: evidence for peripheral gustatory mixture interactions. Brain Res. 727(1-2):79–90.

Formaker BK, MacKinnon BI, Hettinger TP, Frank ME. 1997. Opponent effects of quinine and sucrose on single fiber taste responses of the chorda tympani nerve. Brain Res. 772(1-2):239–242.

Frank ME, Formaker BK, Hettinger TP. 2005. Peripheral gustatory processing of sweet stimuli by golden hamsters. Brain Res Bull. 66(1):70–84.

Grunberg NE. 1982. The effects of nicotine and cigarette smoking on food consumption and taste preferences. Addict Behav. 7(4):317–331.

Grunberg NE. 1985. Nicotine, cigarette smoking, and body weight. Br J Addict. 80(4):369–377.

Haufroid V, Lison D. 1998. Urinary cotinine as a tobacco-smoke exposure index: a minireview. Int Arch Occup Environ Health. 71(3):162–168.

Helgren FJ, Lynch MJ, Kirchmeyer FJ. 1955. A taste panel study of the saccharin off-taste. J Am Pharm Assoc Am Pharm Assoc (Baltim). 44(6):353–355.

Hisatsune C, Yasumatsu K, Takahashi-Iwanaga H, Ogawa N, Kuroda Y, Yoshida R, Ninomiya Y, Mikoshiba K. 2007. Abnormal taste perception in mice lacking the type 3 inositol 1,4,5-trisphosphate receptor. J Biol Chem. 282(51):37225–37231.

Hofmann T, Chubanov V, Gudermann T, Montell C. 2003. TRPM5 is a voltage-modulated and Ca^{2+}-activated monovalent selective cation channel. Curr Biol. 13(13):1153–1158.

Horne J, Lawless HT, Speirs W, Sposato D. 2002. Bitter taste of saccharin and acesulfame-K. Chem Senses. 27(1):31–38.

Huang YJ, Maruyama Y, Dvoryanchikov G, Pereira E, Chaudhari N, Roper SD. 2007. The role of pannexin 1 hemichannels in ATP release and cell-cell communication in mouse taste buds. Proc Natl Acad Sci U S A. 104(15):6436–6441.

Keast R, Breslin P. 2002. An overview of binary taste-taste interactions. Food Qual Prefer. 14:111–124.

Kim SH, Lee Y, Akitake B, Woodward OM, Guggino WB, Montell C. 2010. ***Drosophila*** TRPA1 channel mediates chemical avoidance in gustatory receptor neurons. Proc Natl Acad Sci U S A. 107(18):8440–8445.

Kuhn C, Bufe B, Winnig M, Hofmann T, Frank O, Behrens M, Lewtschenko T, Slack JP, Ward CD, Meyerhof W. 2004. Bitter taste receptors for saccharin and acesulfame K. J Neurosci. 24(45):10260–10265.

Lawless HT. 1977. The pleasantness of mixtures in taste and olfaction. Sensory Processes. 1:227–237.

Li X, Staszewski L, Xu H, Durick K, Zoller M, Adler E. 2002. Human receptors for sweet and umami taste. Proc Natl Acad Sci U S A. 99(7):4692–4696.

Liman ER. 2007. TRPM5 and taste transduction. Handb Exp Pharmacol. 179:287–298.

Liu D, Liman ER. 2003. Intracellular Ca^{2+} and the phospholipid PIP2 regulate the taste transduction ion channel TRPM5. Proc Natl Acad Sci U S A. 100(25):15160–15165.

Liu D, Zhang Z, Liman ER. 2005. Extracellular acid block and acid-enhanced inactivation of the Ca^{2+}-activated cation channel TRPM5 involve residues in the S3-S4 and S5-S6 extracellular domains. J Biol Chem. 280(21):20691–20699.

Liu L, Zhu W, Zhang ZS, Yang T, Grant A, Oxford G, Simon SA. 2004. Nicotine inhibits voltage-dependent sodium channels and sensitizes vanilloid receptors. J Neurophysiol. 91(4):1482–1491.

Luyten T, Bultynck G, Parys JB, De Smedt H, Missiaen L. 2014. Measurement of intracellular Ca^{2+} release in permeabilized cells using $^{45}Ca^{2+}$. In: Parys JB, Bootman MD, Yule DI and Bultynck G, editors. Calcium techniques. A laboratory manual. Cold Spring Harbor: Cold Spring Harbor Laboratory Press. p. 219–224.

Lyall V, Phan TH, Mummalaneni S, Mansouri M, Heck GL, Kobal G, DeSimone JA. 2007. Effect of nicotine on chorda tympani responses to salty and sour stimuli. J Neurophysiol. 98(3):1662–1674.

Meseguer VM, Denlinger BL, Talavera K. 2011. Methodological considerations to understand the sensory function of TRP channels. Curr Pharm Biotechnol. 12(1):3–11.

Misra UK, Gawdi G, Pizzo SV. 1997. Chloroquine, quinine and quinidine inhibit calcium release from macrophage intracellular stores by blocking inositol 1,4,5-trisphosphate binding to its receptor. J Cell Biochem. 64(2):225–232.

Missiaen L, Parys JB, De Smedt H, Himpens B, Casteels R. 1994. Inhibition of inositol trisphosphate-induced calcium release by caffeine is prevented by ATP. Biochem J. 300:81–84.

Missiaen L, Van Acker K, Van Baelen K, Raeymaekers L, Wuytack F, Parys JB, De Smedt H, Vanoevelen J, Dode L, Rizzuto R, *et al.* 2004. Calcium release from the Golgi apparatus and the endoplasmic reticulum in HeLa cells stably expressing targeted aequorin to these compartments. Cell Calcium. 36(6):479–487.

Miyawaki A, Furuichi T, Maeda N, Mikoshiba K. 1990. Expressed cerebellar-type inositol 1,4,5-trisphosphate receptor, P400, has calcium release activity in a fibroblast L cell line. Neuron. 5(1):11–18.

Mojet J, Heidema J, Christ-Hazelhof E. 2004. Effect of concentration on taste-taste interactions in foods for elderly and young subjects. Chem Senses. 29(8):671–681.

Nagatomo K, Kubo Y. 2008. Caffeine activates mouse TRPA1 channels but suppresses human TRPA1 channels. Proc Natl Acad Sci U S A. 105(45):17373–17378.

Oike H, Wakamori M, Mori Y, Nakanishi H, Taguchi R, Misaka T, Matsumoto I, Abe K. 2006. Arachidonic acid can function as a signaling modulator by activating the TRPM5 cation channel in taste receptor cells. Biochim Biophys Acta. 1761(9):1078–1084.

Oliveira-Maia AJ, Stapleton-Kotloski JR, Lyall V, Phan TH, Mummalaneni S, Melone P, Desimone JA, Nicolelis MA, Simon SA. 2009. Nicotine activates TRPM5-dependent and independent taste pathways. Proc Natl Acad Sci U S A. 106(5):1596–1601.

Palade P, Dettbarn C, Volpe P, Alderson B, Otero AS. 1989. Direct inhibition of inositol-1,4,5-trisphosphate-induced Ca^{2+} release from brain microsomes by K^+ channel blockers. Mol Pharmacol. 36(4):664–672.

Parys JB, de Smedt H, Missiaen L, Bootman MD, Sienaert I, Casteels R. 1995. Rat basophilic leukemia cells as model system for inositol 1,4,5-trisphosphate receptor IV, a receptor of the type II family: functional comparison and immunological detection. Cell Calcium. 17(4):239–249.

Peri I, Mamrud-Brains H, Rodin S, Krizhanovsky V, Shai Y, Nir S, Naim M. 2000. Rapid entry of bitter and sweet tastants into liposomes and taste cells: implications for signal transduction. Am J Physiol Cell Physiol. 278(1):C17–C25.

Prawitt D, Monteilh-Zoller MK, Brixel L, Spangenberg C, Zabel B, Fleig A, Penner R. 2003. TRPM5 is a transient Ca^{2+}-activated cation channel responding to rapid changes in $[Ca^{2+}]i$. Proc Natl Acad Sci U S A. 100(25):15166–15171.

Pritchard WS, Robinson JH, Guy TD, Davis RA, Stiles MF. 1996. Assessing the sensory role of nicotine in cigarette smoking. Psychopharmacology (Berl). 127(1):55–62.

Riera CE, Vogel H, Simon SA, Damak S, le Coutre J. 2008. The capsaicin receptor participates in artificial sweetener aversion. Biochem Biophys Res Commun. 376(4):653–657.

Riera CE, Vogel H, Simon SA, le Coutre J. 2007. Artificial sweeteners and salts producing a metallic taste sensation activate TRPV1 receptors. Am J Physiol Regul Integr Comp Physiol. 293(2):R626–R634.

Romanov RA, Rogachevskaja OA, Bystrova MF, Jiang P, Margolskee RF, Kolesnikov SS. 2007. Afferent neurotransmission mediated by hemichannels in mammalian taste cells. EMBO J. 26(3):657–667.

Rose JE, Behm FM, Levin ED. 1993. Role of nicotine dose and sensory cues in the regulation of smoke intake. Pharmacol Biochem Behav. 44(4):891–900.

Sato K, Endo S, Tomita H. 2002. Sensitivity of three loci on the tongue and soft palate to four basic tastes in smokers and non-smokers. Acta Otolaryngol Suppl. 546:74–82.

Schifferstein HN. 2003. Human perception of taste mixtures. In: Doty RL, editor. Handbook of olfaction and gustation. New York: Marcel Dekker. p. 805–822.

Schiffman SS, Booth BJ, Carr BT, Losee ML, Sattely-Miller EA, Graham BG. 1995. Investigation of synergism in binary mixtures of sweeteners. Brain Res Bull. 38(2):105–120.

Simons CT, Boucher Y, Carstens MI, Carstens E. 2006. Nicotine suppression of gustatory responses of neurons in the nucleus of the solitary tract. J Neurophysiol. 96(4):1877–1886.

Sugita M. 2006. Taste perception and coding in the periphery. Cell Mol Life Sci. 63(17):2000–2015.

Talavera K, Gees M, Karashima Y, Meseguer VM, Vanoirbeek JA, Damann N, Everaerts W, Benoit M, Janssens A, Vennekens R, *et al.* 2009. Nicotine activates the chemosensory cation channel TRPA1. Nat Neurosci. 12(10):1293–1299.

Talavera K, Ninomiya Y, Winkel C, Voets T, Nilius B. 2007. Influence of temperature on taste perception. Cell Mol Life Sci. 64(4):377–381.

Talavera K, Yasumatsu K, Voets T, Droogmans G, Shigemura N, Ninomiya Y, Margolskee RF, Nilius B. 2005. Heat activation of TRPM5 underlies thermal sensitivity of sweet taste. Nature. 438(7070):1022–1025.

Talavera K, Yasumatsu K, Yoshida R, Margolskee RF, Voets T, Ninomiya Y, Nilius B. 2008. The taste transduction channel TRPM5 is a locus for bitter-sweet taste interactions. FASEB J. 22(5):1343–1355.

Thebault S, Zholos A, Enfissi A, Slomianny C, Dewailly E, Roudbaraki M, Parys J, Prevarskaya N. 2005. Receptor-operated Ca^{2+} entry mediated by TRPC3/TRPC6 proteins in rat prostate smooth muscle (PS1) cell line. J Cell Physiol. 204(1):320–328.

Tomassini S, Cuoghi V, Catalani E, Casini G, Bigiani A. 2007. Long-term effects of nicotine on rat fungiform taste buds. Neuroscience. 147(3):803–810.

Ullrich ND, Voets T, Prenen J, Vennekens R, Talavera K, Droogmans G, Nilius B. 2005. Comparison of functional properties of the Ca^{2+}-activated cation channels TRPM4 and TRPM5 from mice. Cell Calcium. 37(3):267–278.

Vandenbeuch A, Pillias AM, Faurion A. 2004. Modulation of taste peripheral signal through interpapillar inhibition in hamsters. Neurosci Lett. 358(2):137–141.

Vanlingen S, Parys JB, Missiaen L, De Smedt H, Wuytack F, Casteels R. 1997. Distribution of inositol 1,4,5-trisphosphate receptor isoforms, SERCA isoforms and Ca^{2+} binding proteins in RBL-2H3 rat basophilic leukemia cells. Cell Calcium. 22(6):475–486.

Wilson BS, Pfeiffer JR, Smith AJ, Oliver JM, Oberdorf JA, Wojcikiewicz RJ. 1998. Calcium-dependent clustering of inositol 1,4,5-trisphosphate receptors. Mol Biol Cell. 9(6):1465–1478.

Zhang Y, Hoon MA, Chandrashekar J, Mueller KL, Cook B, Wu D, Zuker CS, Ryba NJ. 2003. Coding of sweet, bitter, and umami tastes: different receptor cells sharing similar signaling pathways. Cell. 112(3):293–301.

Zhang Z, Zhao Z, Margolskee R, Liman E. 2007. The transduction channel TRPM5 is gated by intracellular calcium in taste cells. J Neurosci. 27(21):5777–5786.

Zhao FL, Lu SG, Herness S. 2002. Dual actions of caffeine on voltage-dependent currents and intracellular calcium in taste receptor cells. Am J Physiol Regul Integr Comp Physiol. 283(1):R115–R129.